*Progress In Electromagnetics Research, Vol. 114, 395–405, 2011*

# QUASI-ELLIPTIC FUNCTION BANDPASS FILTER WITH UPPER STOPBAND EXTENSION AND HIGH REJECTION LEVEL USING CROSS-COUPLED STEPPED-IMPEDANCE RESONATORS

**J.-T. Kuo**

Department of Electronic Engineering
Chang Gung University, Taoyuan, Taiwan

**S.-C. Tang and S.-H. Lin**

Institute of Communication Engineering
National Chiao Tung University, Hsinchu, Taiwan

**Abstract**—Planar microstrip filters are designed to have a quasi-elliptic function passband and extended upper stopband with a rejection level of 40 or 50 dB. The design employs stepped-impedance resonators in a compact $2 \times 2$ cross coupled configuration. The geometric parameters of the resonators are planned to shift the third resonance as high as possible, and then the transmission zeros created by the structure are devised to suppress the second resonance, so that a wide upper stopband up to more than 4.5 times the passband frequency can be achieved. By employing the skew-symmetric input/output feeds, three transmission zeros in the frequency band of interest can be created. The leading two zeros are allocated on the both sides of the passband, generating a quasi-elliptic function response with enhanced roll-off rate in the transition bands, and the last zero incorporating with a zero created by anti-coupled-line at higher frequencies are employed to extend the rejection bandwidth. The measurement data agree very well with the simulation responses.

## 1. INTRODUCTION

Bandpass filter is one of the key components in the RF front-end of a wireless transceiver. Due to the increasingly critical demands, the filters are required low cost, compact size, low insertion loss

*Received 10 January 2011, Accepted 4 March 2011, Scheduled 8 March 2011*
Corresponding author: Jen-Tsai Kuo (jtkuo123@mail.cgu.edu.tw).

and sufficiently high rejection in stopband. In the past few decades, parallel-coupled line bandpass filters [1] are one of the most widely used structures; however, this structure suffers from spurious peaks at all harmonics of the passband frequencies [2]. Numerous innovative methods have been proposed to tackle this problem, e.g., [2–4].

Alternatively, the stepped-impedance resonators (SIRs) possess a beautiful resonance characteristic for extending the upper rejection band in bandpass filter design. Its resonance spectrum can be easily adjusted by tuning its geometric parameters, i.e., length and impedance ratios of the high- and low-impedance sections [5]. In [5], an upper stopband with more than 30-dB rejection can be achieved up to 8.2 times the passband frequency. In [6], the impedance ratio of the SIR is increased by etching an aperture in the ground plane under the high-impedance section and printing a floating conductor patch below the low-impedance portion. In this way, the first spurious band of the filter can be significantly pushed up and a meaningful improved out-of-band rejection level can be achieved. In [7, 8], the impedance and length ratios of each constitutive SIR are designed to make identical fundamental frequency, but staggered higher order resonances to achieve multi-spurious suppression The stacked SIR filters in [9] with embedded C-type resonators, aiming at spurious suppression demonstrate a measured rejection level of 54 dB. In [10], double split-end quarter-wave SIRs are devised to construct a sixth-order filter with a bandwidth of 8.5 times the center frequency with at least 37.8 dB of attenuation. In [11], the geometric parameters of the SIRs are tuned to achieve a stopband extended up to 8.16 times passband frequency and an average rejection level better than 25 dB.

In this paper, SIR bandpass filters shown in Fig. 1 are targeted to have not only a quasi-elliptic function passband but also a wide upper stopband with rejection levels of more than 40 or 50 dB. Note that the cross coupled structure features a more compact circuit area than that in [5], where a parallel-coupled structure is used. The two zeros created on both sides of the passband can greatly enhance the frequency selectivity [12, 13], which is an important characteristic in a receiver where image frequency rejection or high band isolation [14] is required. The multimode resonator in [15] composed of half-wave microstrip resonator shunt with radial-line stubs can be synthesized to possess such passbands. The hexagonal bandpass filter with triple-mode resonator in [16] demonstrates a similar passband response. Based on compact miniaturized hairpin resonators, the cross coupled $2 \times 2$ configuration in [17] is also suitable for creating two such zeros. In synthesis, the sign of a specified coupling coefficient has to be opposite to those of the other three. Apparently, the coupling scheme of the

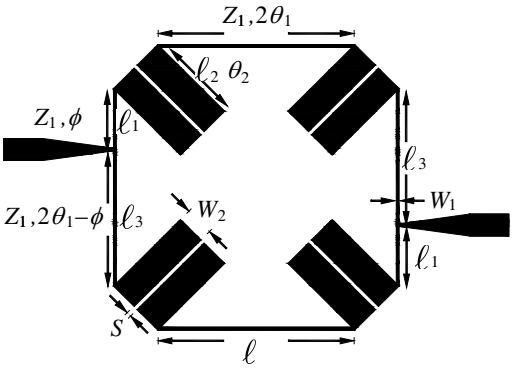


**Figure 1.** Layout of the proposed SIR bandpass filter.

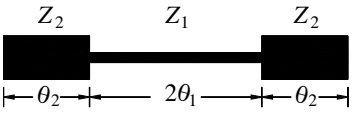


**Figure 2.** Geometry of a SIR.

proposed circuit in Fig. 1 is different from that in [17] although it has the same $2 \times 2$ configuration. This is because that from Fig. 1 the four coupling coefficients will have the same polarities. It will be validated that the creation of the two transmission zeros near the passband of the proposed circuit relies on the skew-symmetric input/output feeds [18] based on the cross coupled configuration. The four anti-parallel-coupled line sections can also generate extra zeros [19] which are used to suppress the higher order resonances of the SIR, so that the upper stopband can be significantly extended.

The paper is organized as follows. Section 2 briefly describes the resonance property of the SIR, and Section 3 formulates the analysis of the transmission zeros generated in the cross coupled structure with skew-symmetric input/output feeds. Section 4 compares the measurement results of two experimental circuits with simulation for validation of the design, and Section 5 draws the conclusion of this work.

## 2. RESONANCE CHARACTERISTICS OF SIR

The SIR in Fig. 2 has two low-impedance ($Z_2$) sections on both sides and a high-impedance ($Z_1$) segment in the middle. The even and odd resonance conditions of the resonator lead to the following equations for calculation of the resonant frequencies:

$$\tan\theta_1 = R\cot\theta_2 \tag{1a}$$

$$R\tan\theta_1 = -\tan\theta_2 \tag{1b}$$

where $Z_1$ and $Z_2$ are characteristic impedances $\theta_1$ and $\theta_2$ are electrical lengths of the segments, and $R = Z_2/Z_1$ is defined as the impedance

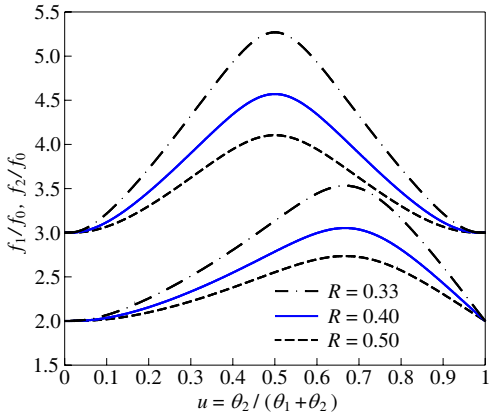


**Figure 3.** Normalized resonance spectrum of a SIR with $R = 0.33$, 0.4, and 0.5. $f_0$, $f_1$ and $f_2$ denote the first, the second and the third resonance frequencies, respectively.

ratio. Fig. 3 plots normalized spectrum for a SIR with $R = 0.33$, 0.4 and 0.5 against the length ratio $u = \theta_2/(\theta_1 + \theta_2)$. The second ($f_1$) and the third ($f_2$) resonance frequencies are normalized with respect to the first one ($f_0$). It can be seen that the maxima of $f_1/f_0$ and $f_2/f_0$ occur at $u = 0.67$, and 0.5, respectively.

## 3. ANALYSIS

Figure 4 shows the transmission line model for analysis of the proposed circuit in Fig. 1. There are two signal paths from the input to output. The coupling between the source and load are established by the tapped input/output structure, so that the $Z_1$-segment of the input/output resonator has to be divided into two parts in the model. The matrices $[M_1]$, $[M_3]$ and $[M_5]$ represent $ABCD$ matrices for a section of transmission line, so they share the same forms. For example,

$$[M_1] = \begin{bmatrix} \cos\phi & jZ_1 \sin\phi \\ jY_1 \sin\phi & \cos\phi \end{bmatrix} \tag{2}$$

where $Y_1 = Z_1^{-1}$ and $\phi$ is used to represent the tap position in terms of phase angle at the passband frequency. The matrices $[M_2]$ and $[M_4]$ denote the $ABCD$ parameters of an anti-parallel-coupled line. It can be shown that

$$[M_2] = \frac{Z_s}{Z_d} \begin{bmatrix} 1 & -j\frac{2Z_{oe}Z_{oo}}{Z_s} \cot\theta_2 \\ j\frac{2}{Z_s} \tan\theta_2 & 1 \end{bmatrix} \tag{3}$$

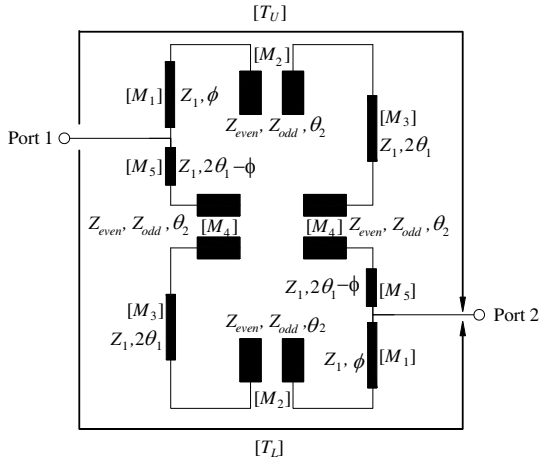


**Figure 4.** Transmission line analysis of the proposed cross-coupled SIR filter.

where $Z_s = Z_{oe} + Z_{oo}$, $Z_d = Z_{oe} - Z_{oo}$, and $Z_{oe}$ and $Z_{oo}$ are the even and odd mode characteristic impedances, respectively, of the coupled line. In this equation, the even and odd modal phase velocities are assumed identical.

The transmission and reflection properties of the two paths can be represented by $2 \times 2$ transmission matrices $[T_U]$ and $[T_L]$, which can be obtained by successively multiplying the constitutive $ABCD$ matrices along each path:

$$[T_U] = [M_1][M_2][M_3][M_4][M_5] \tag{4a}$$

$$[T_L] = [M_5][M_4][M_3][M_2][M_1] \tag{4b}$$

To simplify the notation, all $ABCD$ matrices are temporarily derived with $Z_1 = 1\,\Omega$, we have

$$[M_1] = \cos\phi \begin{bmatrix} 1 & j\tan\phi \\ j\tan\phi & 1 \end{bmatrix} = \cos\phi \left( \begin{bmatrix} 1 & 0 \\ 0 & 1 \end{bmatrix} + j\tan\phi \begin{bmatrix} 0 & 1 \\ 1 & 0 \end{bmatrix} \right) \tag{5}$$

Then, the matrix product $[M_1]$ $[M_2]$ can be written in a form as

$$[M_1] \begin{bmatrix} 1 & b \\ c & 1 \end{bmatrix} = \cos\phi \left( \begin{bmatrix} 1 & b \\ c & 1 \end{bmatrix} + j\tan\phi \begin{bmatrix} c & 1 \\ 1 & b \end{bmatrix} \right) \tag{6}$$

where $b$ and $c$ stand for the matrix entries in (3). Note that the second matrix in the parentheses is the first one with two interchanged rows. The products $[M_3]$ $[M_4]$ and the matrix post-multiplied by $[M_5]$ can be obtained in a similar fashion. In this way, the successive matrix multiplication in (4a) can be performed with a minimal effort.

In (4), the order of the successive multiplication of the sub-matrices of $[T_L]$ is just reverse of that of $[T_U]$. Based on the network theory, one can prove that $A_U = D_L$, $B_U = B_L$, $C_U = C_L$ and $D_U = A_L$, where the subscripts $U$ and $L$ represent the upper path and lower path, respectively. The $S$-parameters of the entire circuit can be obtained by converting the sum of the $Y$-parameter matrices of the two paths, which can be derived from $[T_U]$ and $[T_L]$. Thus, the transmission coefficient $S_{21}$ can be derived as

$$S_{21} = \frac{4B_U Y_o}{(A_U + D_U + B_U Y_o)^2 - 4} \tag{7}$$

where $Y_o$ is the reference port admittance. Based on (5) and (6), the related entries in $[T_U]$ can be easily derived as follows:

$$\frac{Z_d^2}{Z_s^2} \times (A_U + D_U) = 2\cos 4\theta_1 + 2bc - \alpha^2 \sin^2 2\theta_1 + 2j\alpha \sin 4\theta_1 \tag{8a}$$

$$\frac{Z_d^2}{Z_s^2} \times B_U = \alpha \cos 4\theta_1 + \beta \cos 2\theta_1 \cos(2\theta_1 - 2\phi) + j\frac{\sin 2\theta_1}{2}\left[(\alpha+4)\cos 2\theta_1 + \alpha\beta \cos(2\theta_1 - 2\phi)\right] \tag{8b}$$

where $\alpha = bZ_1 + cY_1$ and $\beta = bZ_1 - cY_1$, when the normalization impedance $Z_1$ is taken back to the formulation. Fig. 5 plots variation of the zeros versus $\phi/\theta_1$ obtained by enforcing $S_{21} = 0$. Obviously, from (7) and (8) the transmission zeros of the proposed circuit fall into two categories; one is due to $B_U = \infty$ or $A_U + D_U = \infty$, and the other is $B_U = 0$. The former two conditions occur when $b \to \infty$ or $c \to \infty$, or $\sin\theta_2 \cos\theta_2 = 0$. This means that the zero is resulted from the open-ended anti-parallel-coupled line, and is independent of $\phi$, as denoted as $f_{z3}$ in Fig. 5. This is because that from Fig. 1 both the open-ended anti-parallel-coupled lines $[M_2]$ and $[M_4]$ are series elements of the upper and lower paths. It is possible to create two transmission zeros by making $\theta_2$ in $[M_2]$ and $[M_4]$ different; however, in order to enhance the rejection in the stopband, the dimensions of the two open-ended anti-parallel-coupled lines $[M_2]$ and $[M_4]$ are made identical. This is because a single transmission zero usually has an insufficient bandwidth for suppression of the spurious resonance [5]. When inequality or dispersion of the modal phase velocities are considered, more electromagnetic simulations will be required [19]. Based on the resonance spectrum in Fig. 3, the first spurious $f_1$ has to be cancelled and the second spurious $f_2$ has to be pushed as far away as possible. Thus, $f_{z3}$ has to coincide with $f_1$ and length ratio $u = 0.5$ be chosen.

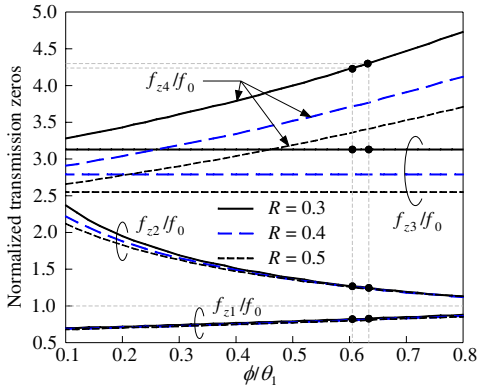


**Figure 5.** Normalized transmission zeros of the circuit versus $\phi/\theta_1$.

The zeros of the proposed circuit obtained by solving $B_U = 0$ are from the tap position and the cross coupled configuration. In filter synthesis, the value of $\phi$ should match the circuit bandwidth with the singly loaded $Q$ of the input and output resonators, and the derived formula for SIRs can be referred to [5]. From (8b), however, $Z_{oe}$, $Z_{oo}$, $Z_1$, $\theta_1$ and $\theta_2$ are also the key factors for determining the zeros. As a result, a total of three transmission zeros by $B_U = 0$ can be utilized in this design. As shown in Fig. 5, when the impedance ratio $R$ is changed from 0.3 to 0.5, $f_{z1}$ and $f_{z2}$ have only small changes, but $f_{z4}$ may vary significantly. The two leading zeros $f_{z1}$ and $f_{z2}$ can be used as the zero transmission frequencies on both sides of the passband at $f_0$ to form a quasi-elliptic function passband, and the fourth zero $f_{z4}$ can be used to enhance the rejection levels in the stopband.

## 4. SIMULATION AND MEASUREMENT

Two experimental circuits are fabricated and measured to validate the above analysis. The first experimental circuit is built on a Rogers RO4003 substrate of which the relative dielectric constant $\varepsilon_r = 3.38$ and thickness $h = 0.508\,\text{mm}$. The filter is designed to have center frequency $f_0 = 2.45\,\text{GHz}$ and a fractional bandwidth $\Delta = 10\%$. Fig. 6(a) plots the simulated and measured responses. The simulation is done by the electromagnetic simulation software package IE3D [20], and the measurement is performed using an Angilent E8364B Network Analyzer. The SIRs have $R = 0.3$ and other electrical parameters at $f_0$ are $2\theta_1 = 55.78°$, $Z_1 = 115.05\,\Omega$, $\phi = 16.90°$, $\theta_2 = 27.67°$, $Z_{oe} = 39.56\,\Omega$ and $Z_{oo} = 28.08\,\Omega$. The simulated and measured passband insertion losses are 1.55 dB and 1.74 dB, respectively. The

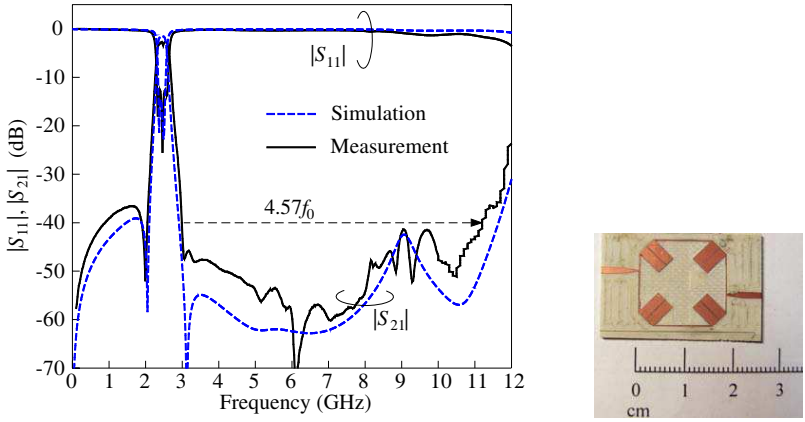


**Figure 6.** Performance of the first synthesized circuit. (a) Simulation and measurement $|S_{11}|$ and $|S_{21}|$ responses. (b) Photograph of the experimental circuit. Geometric parameters (See also Fig. 1): $\ell = 12.295\,\text{mm}$, $W_1 = 0.2\,\text{mm}$, $\ell_1 = 3.78\,\text{mm}$, $\ell_2 = 5.7\,\text{mm}$, $\ell_3 = 8.515\,\text{mm}$, $W_2 = 1.99\,\text{mm}$, $S = 0.18\,\text{mm}$.

two transmission zeros near the passband at 2.03 and 3.02 GHz can be observed In measurement, the upper stopband with a rejection level better than 40 dB can be extended up to 11.2 GHz, or $4.57f_0$. It can be observed that the measured data agree well with the simulation responses. Fig. 6(b) shows the photograph of the measured circuit.

Both the simulation and measurement $|S_{21}|$ curves in Fig. 6(a) present a hump of $-40\,\text{dB}$ at 9 GHz or $3.67f_0$. In the neighborhood of this frequency, based on Fig. 3 the spurious peaks are at 7.67 GHz ($f_1/f_0 = 3.13$) and 12.9 GHz ($f_2/f_0 = 5.27$). Now that the former unwanted peak has been successfully cancelled by $f_{z3}$, the rise of the hump should be a part of skirt of the SIR resonances at $f_2$. Although the zero $f_{z4}$ created by the cross coupled configuration at $4.23f_0 = 10.4\,\text{GHz}$ is believed to have a significant contribution to the stopband extension the hump can still be expected to be even lower since $f_{z3}$ generated by the anti-coupled-line is a second-order zero. Thus, a second experiment circuit is designed at $f_0 = 1\,\text{GHz}$ and fabricated on a Duroid 5880 substrate with a relative dielectric constant $\varepsilon_r = 2.2$ and thickness $h = 0.508\,\text{mm}$. The fractional bandwidth $\Delta = 12\%$. The electrical parameters of the measured circuit at $f_0$ are $2\theta_1 = 55.68^\circ$, $Z_1 = 136.3\,\Omega$, $\phi = 17.66^\circ$, $\theta_2 = 27.63^\circ$, $Z_{oe} = 46.67\,\Omega$ and $Z_{oo} = 33.05\,\Omega$. Fig. 7(a) plots the simulated and measured $|S_{11}|$ and $|S_{21}|$ responses. The simulated and measured in-band insertion losses are 2.5 and 2.7 dB, respectively. The two transmission zeros

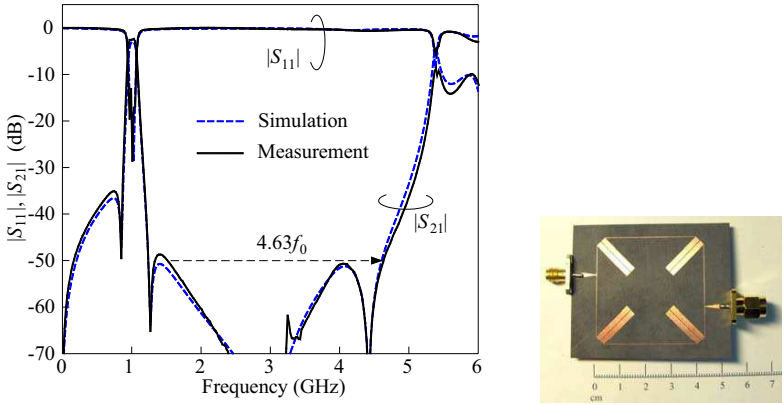


**Figure 7.** Performance of the second experimental filter. (a) Simulation and measurement $|S_{11}|$ and $|S_{21}|$ responses. (b) Photograph of the measured circuit. Geometric parameters: $\ell = 35.46\,\text{mm}$, $W_1 = 0.2\,\text{mm}$, $\ell_1 = 11.15\,\text{mm}$, $\ell_2 = 16.78\,\text{mm}$, $\ell_3 = 24.12\,\text{mm}$, $W_2 = 2.08\,\text{mm}$, $S = 0.2\,\text{mm}$.

on the both sides of the passband are realized at 0.85 and 1.27 GHz. The experimental filter shows roll-off rates better than 300 dB/GHz due to the two transmission zeros on both sides of the passband. It can be observed that an upper stopband up to $4.63f_0$ is obtained even when a rejection level of 50 dB is referenced. Comparing with the $|S_{21}|$ response in Fig. 6, one can observe that the rejection levels around $f_{z3}$ and $f_{z4}$ are significantly improved. This could be due to that this substrate has less dispersion effects (lower operation frequencies and $\varepsilon_r$) and loss ($\tan\delta = 0.0004$) than that used in Fig. 6 ($\tan\delta = 0.0027$). Fig. 7(b) shows the photograph of the experimental circuit.

## 5. CONCLUSION AND DISCUSSION

Compact cross-coupled stepped-impedance resonators (SIRs) bandpass filters with a quasi-elliptic function passband and wide upper stopband are synthesized and implemented. The two transmission zeros near passband are created by a proper I/O feed structure and can be synchronously tuned by changing the tap position. In addition, the transmission zero due to the four anti-parallel-coupled lines greatly suppress the first spurious of the SIR; therefore, a wide upper stopband up to around $4.6f_0$ can be realized with rejection levels better than 50 dB. The measurement results of the fabricated experimental circuit agree very well with the simulation data and validate the design idea.

Changing the impedance ratio of the SIR can be an effective way for extending the upper stopband, provided that the circuit size and the radiation loss can be compromised. In addition, creating more transmission zeros can be necessary for achievement of a high rejection level, e.g., up to 50 dB, over a wide upper stopband, since a single transmission zero is limited its relative narrow bandwidth.

## ACKNOWLEDGMENT

This work was supported by the National Science Council, Taiwan, under Grant NSC 98-2211-E-009-032-MY2.

## REFERENCES

1. Pozar, D. M., *Microwave Engineering*, 3rd edtion, Wiley, New York, 2005.
2. Kuo, J.-T. and M.-H. Wu, "Corrugated parallel-coupled line bandpass filters with multispurious suppression," *IET — Microwaves, Antennas, and Propagation*, Vol. 1, No. 3, 718–722, Jun. 2007.
3. Kuo, J.-T., S.-P. Chen, and M. Jiang, "Parallel-coupled microstrip filters with over-coupled end stages for suppression of spurious responses," *IEEE Micow. Wirelss Compon. Lett.*, Vol. 13, No. 10, 440–442, Oct. 2003.
4. Kuo, J.-T. and H.-P. Lin, "Dual-band bandpass filter with improved performance in extended upper rejection band," *IEEE Trans. Microw. Theory Tech.*, Vol. 57, No. 4, 824–829, Apr. 2009.
5. Kuo, J.-T. and E. Shih, "Microstrip stepped-impedance resonator bandpass filter with an extended optimal rejection bandwidth," *IEEE Trans. Microw. Theory Tech.*, Vol. 51, No. 5, 1554–1559, May 2003.
6. Velazquez-Ahumada, M. D. C., J. Martel, F. Medina, and F. Mesa, "Design of a bandpass filter using stepped-impedance resonators with floating conductors," *Progress In Electromagnetics Research*, Vol. 105, 31–48, 2010.
7. Chen, C.-F., T.-Y. Huang, and R.-B. Wu, "Design of microstrip bandpass filters with multiorder spurious-mode suppression," *IEEE Trans. Microw. Theory Tech.*, Vol. 53, No. 12, 3788–3793, Dec. 2005.
8. Lin, S. C., P.-H. Deng, Y.-S. Lin, C.-H. Wang, and C.-H. Chen, "Wide-stopband microstrip bandpass filters using dissimilar

quarter-wavelength stepped-impedance resonators," *IEEE Trans. Microw. Theory Tech.*, Vol. 54, No. 3, 1011–1018, Mar. 2006.

9. Tang, C.-W. and H.-H. Liang, "Parallel-coupled stacked SIRs bandpass filters with open-loop resonators for suppression of spurious responses," *IEEE Micow. Wirelss Compon. Lett.*, Vol. 15, No. 11, 802–804, Nov. 2005.
10. U-yen, K., E. J. Wollack, T. A. Doiron, J. Papapolymerou, and J. Laskar, "A planar bandpass filter design with wide stopband using double split-end stepped-impedance resonators," *IEEE Trans. Microw. Theory Tech.*, Vol. 54, No. 3, 1237–1244, Mar. 2006.
11. Wu, H.-W., S.-K. Liu, M.-H. Weng, and C.-H. Hung, "Compact microstrip bandpass filter with multispurious suppression," *Progress In Electromagnetics Research*, Vol. 107, 21–30, 2010.
12. Dai, G.-L. and M.-Y. Xia, "Novel miniaturized bandpass filters using spiral-shaped resonators and window feed structures," *Progress In Electromagnetics Research*, Vol. 100, 235–243, 2010.
13. Wen, S. and L. Zhu, "Numerical synthesis design of coupled resonator filters," *Progress In Electromagnetics Research*, Vol. 92, 333–346, 2009.
14. Huang, C.-Y., M.-H. Weng, C.-S. Ye, and Y.-X. Xu, "A high band isolation and wide stopband diplexer using dual-mode stepped-impedance resonators," *Progress In Electromagnetics Research*, Vol. 100, 299–308, 2010.
15. Zhang, L., Z.-Y. Yu, and S.-G. Mo, "Novel planar multimode bandpass filters with radial-line stubs," *Progress In Electromagnetics Research*, Vol. 101, 33–42, 2010.
16. Mo, S.-G., Z.-Y. Yu, and L. Zhang, "Design of triple-mode bandpass filter using improved hexagonal loop resonator," *Progress In Electromagnetics Research*, Vol. 96, 117–125, 2009.
17. Kuo, J.-T., M.-J. Maa, and P.-H. Lu, "A microstrip elliptical function filter with compact miniaturized hairpin resonators," *IEEE Microw. Guided Wave Lett.*, Vol. 10, No. 3, 94–95, Mar. 2000.
18. Tsai, C.-M., S.-Y. Lee, and C.-C. Tsai, "Performance of a planar filter using a 0° feed structure," *IEEE Trans. Microw. Theory Tech.*, Vol. 50, No. 10, 2362–2367, Oct. 2002.
19. Tsai, C.-M., S.-Y. Lee, and H.-M. Lee, "Transmission-line filters with capacitively loaded coupled lines," *IEEE Trans. Microw. Theory Tech.*, Vol. 51, No. 5, 1517–1524, May 2003.
20. IE3D simulator, Zeland Software Inc., Jan. 2002.